Diagnosis of turbulence radiation interaction in turbulent flames and implications for modeling in Large Eddy Simulation

D. Poitou[*], **B. Cuenot**[**], **M. El Hafi**[***]
[*]**poitou@enstimac.fr,** [**]**cuenot@cerfacs.fr,** [***]**elhafi@enstimac.fr**

Abstract

An *a priori* study of the turbulence radiation interaction (TRI) is performed on numerical data from Direct Numerical Simulation (DNS) of a turbulent flame. The influence of the various correlations that appear in the radiative emission is investigated and their impact is evaluated in the context of Large Eddy Simulation (LES). In LES, only filtered quantities are computed, where the filter is the grid. The radiative emission is reconstructed first from the exact, then filtered solution variables and the sensitivity to the filter size is evaluated. Three approaches are used to take into account the subgrid scale correlations : the no-TRI, partial TRI and full TRI approaches. Results show that the full TRI is exact compared to the reference emission and that the partial TRI performs worse than the no-TRI. This indicates that in the studied case, the TRI must be considered in LES in a full formulation.

1   Introduction

Turbulence is one of the most common state of fluid flows, either in industrial applications or natural phenomena. They develop for example when the Reynolds number $Re = UL/\nu$ (where U is the flow velocity, L is a flow charateristic length and ν is the viscosity), reaches sufficiently high values. Although the general equations of fluid dynamics allow to describe both turbulent and laminar flows, computational constraints limit their resolution and different approaches may be used. Direct numerical simulation (DNS) reproduces exactly the turbulent flow but due to a high CPU cost it is restricted to simple geometries and moderate Re. On the contrary Reynolds-Average-Navier-Stokes (RANS) simulations are very fast and handle complex high Re flows, but compute only mean solutions of steady flows. The introduction of Large Eddy Simulations (LES) gives access to filtered variables in high Re, non stationary complex turbulent flows. However it still requires modeling for the subgrid scale phenomena. In all these simulations the radiative transfer is often omitted because of its complexity and prohibitive calculation time. Nevertheless the concerns about energy savings and environment safeguarding impose significant increase of efficiency and decrease of pollutant emissions. As the production of polluting species, like nitrogen oxide (NO_x) and soot, is known to be very sensitive to temperature levels, radiation has now become a key point in modern combustion simulations.

The importance of turbulence-radiation interaction (TRI) is by now well recognized in the scientific community. This observation is supported by experimental studies, conducted mostly by Faeth and Gore and theirs co-workers over the last twenty years for a number of fuels ([1, 2, 3, 4, 5]). This experimental data demonstrate that, depending on the fuel, the radiative emission of a turbulent flame may be up to 50 to 300% higher than it would be evaluated from the mean values of temperature and absorption coefficient.

Theoretical studies provide an additional support for the importance of TRI in combustion applications. Cox (1977) [6] shows that the temperature fluctuations may increase the radiative

emission by 100% if the level of fluctuation exceeds 41%. He also suggests that the turbulent fluctuations may affect the absorption coefficient leading to an increase of flame emission. Kabashnikov and Kmit (1979) [7] and Kabashnikov and Myasnikova (1985) [8] formalized the optically thin eddy approximation (OFTA) commonly used for closure models in TRI. They conclude that TRI may increase the radiative intensity by a factor two or three.

In addition, numerous numerical studies have been carried out to demonstrate the effects of TRI and to evaluate the impact of different parameters [9]. In uncoupled calculations, the radiative transfer is computed from the temperature and species concentrations provided by experiment or combustion simulation results. The fluctuations are commonly generated by stochastic models. Predictions using stochastic models give results in good agreement with experimental data. With this approach Grosshandler [10, 11] shows that TRI may increase the radiative intensity by a factor two. In the case of very sooty flames the emission may decrease because of the negative cross-correlation between soot volumetric fraction and temperature. Jeng [12] points out that TRI is weak in carbon monoxide/air flames (in order of 10%), moderate in methane/air flames (in order of 10% to 30%) and important in hydrogen/air flames (in order of 100%). Kounalakis, Faeth, Sivathanu, Zheng [13, 14] or Coelho [15] also give results in agreement with an increase of radiative emission by TRI. Coupled calculations show that TRI contributes to lower the flame temperature and increase the wall fluxes. Adams and Smiths [16] report temperature reductions by 50K to 100K. These results are confirmed by the work of Modest [17] also showing that wall fluxes may increase by 40%. Coelho [18] finds that the radiative heat loss may increase by 50% if taking into account all TRI effects.

DNS is a powerful tool to diagnose different effects of TRI and to test usual approximations like the OFTA. It was used recently by Wu [19] to study TRI in the context of RANS, to evaluate the effect of the deviation from the mean of the solution variables. In LES, only the subgrid part of the fluctuations is unknown and it is a deviation from the local filtered value. Therefore the impact of TRI might be very different and it is the purpose of the present work to analyse it using the same methodology: the radiation calculations are performed as a post-processing treatment of available DNS results [20], i.e. in an uncoupled approach. In the following, section 2 gives the basic theoretical elements of the analysis, section 3 describes the configuration and the radiation calculations, and finally section 4 presents the results.

2 Turbulence radiation interaction

2.1 LES of turbulent flows

Turbulence is a complex phenomenon involving non-linear processes and developing over a wide range of spatial and temporal scales. In industrial applications it is characterized by the Reynolds number introduced above and some particular length scales such as the integral length scale l_e corresponding to the largest flow structures or the Kolmogorov scale η associated to the smallest eddies. In the LES description of turbulence, a low-pass filter is used to decompose turbulent quantities into two parts [21]:

$$X = \overline{X} + X'$$ (1)

where $\overline{X}$ is the filtered value and X' is the fluctuation. The filtered value is obtained by applying a spatial filter H [22]:

$$\overline{X}(x) = \int_D H(x - x')X(x)dx'$$ (2)

where x is the spatial location vector. The filter is characterized by a size Δ. In practice the filter is the grid itself and Δ is directly linked to the mesh size. Note that in general $\overline{\overline{X}} \neq \overline{X}$ and $\overline{X'} \neq 0$. These relationships are only true if the filter is a cut-off filter in the spectral space. However, as will be seen later, they are usually assumed to allow model derivations, but it will be also shown that the induced error is weak.

2.2 Radiative transfer

In a non-scattering and non-reflecting medium, the differential form of the radiative transfer equation is :

$$\frac{\partial I_\nu}{\partial t} + \frac{\partial I_\nu}{\partial s} = \kappa_\nu \left(I_{b\nu} - I_\nu \right) \tag{3}$$

with $I_\nu(x,t)$ the radiative intensity by solid angle, $I_{b\nu}$ the blackbody radiation intensity, κ_ν the spectral absorption coefficient and s the curvilinear coordinate along the line of sight.

Spectral model

To take into account the spectral dependence of the radiative properties, several approaches are possible, listed here from the simplest to the highest complexity (and CPU cost): global models (gray gas or weighted sum of gray gases), narrow bands models and finally line-by-line models. In the context of combustion applications, obviously line-by-line models are the most accurate but they have a prohibitive CPU cost. On the other hand global models are not accurate enough in case of non-homogeneous and non-isothermal medium. In a combustion chamber the radiant species being able to contribute to the radiation are H_2O, CO_2 and should be included.

Therefore the Malkmus model using narrow bands represents the best compromise between accuracy and rapidity in this context. The average transmittivity for a narrow band $\Delta\nu$ of a gas thickness layer l is expressed as :

$$\langle T \rangle_{\Delta\nu}(l) = exp\left[\Phi \left(1 + \left(1 + \frac{2 \langle \kappa \rangle_{\Delta\nu} l}{\Phi} \right)^{1/2} \right) \right] \tag{4}$$

where $\langle \kappa \rangle_{\Delta\nu}$ is the average value of the absorption coefficient over the narrow band, and Φ is the shape parameter.

Data for $(\langle \kappa \rangle_{\Delta\nu}, \Phi)$ were taken from the spectroscopic database of Taine and Soufiani [23], that gives values for temperatures between 300K and 2900K and for 367 bands of widths $\Delta\nu = 25$ cm^{-1}. In order to take into account the mixture composition several models are proposed by Liu and al [24]. The one chosen has the main adventage to insure a good compromise between accuracy CPU time and is based on the optically thin limit, it provide $\langle \kappa_{mix} \rangle$ and Φ_{mix} for a mixture of N_{gas} of parameters κ_n and Φ_n:

$$\langle \kappa_{mix} \rangle_{\Delta\nu} = \sum_{n=1}^{N_{gas}} \langle \kappa_n \rangle_{\Delta\nu} \text{ and } \frac{\langle \kappa_{mix} \rangle_{\Delta\nu}^2}{\Phi_{mix}} = \sum_{n=1}^{N_{gas}} \frac{\langle \kappa_n \rangle_{\Delta\nu}^2}{\Phi_n} \tag{5}$$

The spectral dependence of κ is reconstructed from the above average quantities by the k-distribution method that consists in using a distribution function of the absorption coefficients $f(\kappa)$ [25]. The average transmitivity on a narrow band is written as :

$$\langle T \rangle_{\Delta\nu}(l) = \int_0^\infty exp(-\kappa l) f(\kappa) d\kappa \tag{6}$$

It is possible to determine $f(\kappa)$ by observing that $\langle T \rangle_{\Delta \nu}$ is the Laplace transform of f :

$$f(\kappa) = T.L.^{-1}\left(\langle T \rangle_{\Delta \nu}(l)\right) \tag{7}$$

In general $f(\kappa)$ is not monotonous and two different values of κ may correspond to the same value of f. It is more convenient to introduce the cumulative sum of the probability density function :

$$g(\kappa) = \int_0^\kappa f(\kappa')d\kappa' \tag{8}$$

This function is now bijective and defined in the interval [0,1], which makes it easy to inverse.

In addition for non-homogeneous and anisotherm media it is necessary to use the so-called assumption of correlated-k, stating that the variations of pressure and temperature on the optical paths do not modify the spectrum or only in a uniform way, this approximation could be used in this application.

To inverse the function $g(\kappa)$ a method developed in [26] based on tabulated values and linear interpolations is used. In this method the coefficients $h_{i,j}$, tabulated as functions of the discretized Φ_i (over N_{quad} points) and for each spectral band j, allow to calculate $\kappa_{mix(i,j)}$ as:

$$\kappa_{mix(i,j)} = h_{i,j}(\Phi_{mix,i}) \langle \kappa_{mix} \rangle_{\Delta \nu_j} \tag{9}$$

Finally, to calculate the Planck absorption coefficient (13), the integral over each narrow band is calculated:

$$\kappa_P = \frac{\pi}{\sigma T^4} \int_0^\infty \kappa_\nu I_{b\nu} d\nu = \sum_{i=1}^{N_{quad}} \sum_{j=1}^{N_{band}} w_i \kappa_{mix,ij} \langle L_b \rangle_{\Delta \nu_j} \Delta \nu_j \tag{10}$$

In the above expression, $\langle L_b \rangle_{\Delta \nu_j}$ represents the mean Planck function over the narrow band j of width $\Delta \nu$.

Radiative flux

The divergence of the radiative flux $\mathbf{q}$ is written as :

$$\nabla \cdot \mathbf{q} = \int_0^{+\infty} \kappa_\nu \left(4\pi I_{b\nu} - G_\nu\right) d\nu \tag{11}$$

where $G_\nu = \int_{4\pi} I_\nu d\Omega$ is the direction-integrated incident radiation. By integrating over frequencies, one obtains:

$$\nabla \cdot \mathbf{q} = 4\sigma \kappa_P T^4 - \int_0^{+\infty} \kappa_\nu G_\nu d\nu \tag{12}$$

with $\int_0^\infty I_{b\nu} d\nu = \sigma T^4/\pi$ (σ being the Stephan constant), and introducing the mean Planck absorption coefficient :

$$\kappa_P = \frac{\int_0^\infty \kappa_\nu I_{b\nu} d\nu}{\int_0^\infty I_{b\nu} d\nu} = \frac{\pi}{\sigma T^4} \int_0^\infty \kappa_\nu I_{b\nu} d\nu \tag{13}$$

2.3 Radiative transfer in turbulent flames

To study the radiative transfer and TRI in turbulent flames in the LES context, the filtered form of the radiative source term is investigated. By definition :

$$\overline{\nabla \cdot \mathbf{q}} = 4\sigma \overline{\kappa_P T^4} - \int_0^{+\infty} \overline{\kappa_\nu G_\nu} d\nu \tag{14}$$

Usually in DNS calculations, the quantity $\kappa_P L$, where L is the length of the domain, is small and the medium is optically thin. In the studied case for example $\kappa_P L = 10$ m^{-1} x 3 mm $= 310^{-2}$. By considering the optically thin approximation (absorption in the medium is negligible), absorption exchanges occur mainly with the walls so that Eq. (14) reduces to :

$$\overline{\nabla \cdot \mathbf{q}} = 4\sigma \overline{\kappa_P T^4} - \overline{\kappa_P} T_\infty^4 = \nabla \cdot q_E - \nabla \cdot q_A \tag{15}$$

where T_∞ is the wall temperature. This approximation is commonly made in combustion applications, and fairly valid for small-scale non-luminous flames. Finally correlations of fluctuating quantities appear only in the emission term $\nabla \cdot q_E$ and the term $\nabla \cdot q_A$ is not investigated in the following.

The emission part of (14) reveals a correlation between the absorption coefficient and the fourth power of temperature. Using the decomposition of (1) for κ_P, one gets:

$$\overline{\kappa_P T^4} = \overline{\kappa_P} \overline{T^4} + \overline{\kappa_P' T^4} \tag{16}$$

where it is supposed that $\overline{\overline{\kappa_P}} = \overline{\kappa_P}$ and $\overline{\overline{T^4}} = \overline{T^4}$. This allows to introduce two terms R_{T^4} and R_{I_b} as :

$$\overline{\kappa_P T^4} = \overline{\kappa_P} \overline{T}^4 \left(\frac{\overline{T^4}}{\overline{T}^4} + \frac{\overline{\kappa_P' T^4}}{\overline{\kappa_P} \overline{T}^4} \right) = \overline{\kappa_P} \overline{T}^4 \left(R_{T^4} + R_{I_b} \right) \tag{17}$$

These two distinct correlations, R_{T^4} and R_{I_b} indicate respectively the temperature auto-correlation and the cross-correlation between temperature and absorption coefficient. Introducing now temperature fluctuations, and assuming that $\overline{\kappa_P'} = \overline{(T^4)'} = 0$, it is possible to develop the two contributions as:

$$R_{T^4} = 1 + 6\frac{\overline{T'^2}}{\overline{T}^2} + 4\frac{\overline{T'^3}}{\overline{T}^3} + \frac{\overline{T'^4}}{\overline{T}^4} \tag{18}$$

$$R_{I_b} = 4\frac{\overline{\kappa_P' T'}}{\overline{\kappa_P} \cdot \overline{T}} + 6\frac{\overline{\kappa_P' T'^2}}{\overline{\kappa_P} \cdot \overline{T}^2} + 4\frac{\overline{\kappa_P' T'^3}}{\overline{\kappa_P} \cdot \overline{T}^3} + \frac{\overline{\kappa_P' T'^4}}{\overline{\kappa_P} \cdot \overline{T}^4} \tag{19}$$

Assuming that the intensity of fluctuations is low, correlations of higher order than two may be dropped, leading to:

$$R_{T^4} \approx 1 + 6\frac{\overline{T'^2}}{\overline{T}^2} \text{ and } R_{I_b} \approx 4\frac{\overline{\kappa_P' T'}}{\overline{\kappa_P} \cdot \overline{T}} + 6\frac{\overline{\kappa_P' T'^2}}{\overline{\kappa_P} \cdot \overline{T}^2} \tag{20}$$

Assuming that the impact of species concentration fluctuations is negligible on κ_P, a second-order Taylor expansion of $\kappa_P(T) = \kappa_P(\overline{T} + T')$ is performed :

$$\kappa_P(T) = \kappa_P(\overline{T}) + T' \left(\frac{\partial \kappa_P}{\partial T} \right)_{\overline{T}} + \frac{T'^2}{2} \left(\frac{\partial^2 \kappa_P}{\partial T^2} \right)_{\overline{T}} + ... \tag{21}$$

and after filtering :

$$\overline{\kappa_P(T)} = \kappa_P(\overline{T}) + \frac{\overline{T'^2}}{2} \left(\frac{\partial^2 \kappa_P}{\partial T^2} \right)_{\overline{T}} + ... \tag{22}$$

Multiplying $\kappa_P - \overline{\kappa_P} = \kappa'_P$ (from (21) and (22)), by T' and filtering, one finally obtains (at the second order) :

$$R_{I_b} \approx 4 \frac{\overline{T'^2}}{\overline{\kappa_P} \overline{T}} \left(\frac{\partial \kappa_P}{\partial T} \right)_{\overline{T}} \tag{23}$$

Not surprisingly, the cross-correlation between T and κ_P is expressed through the derivative $\partial \kappa_P / \partial T$.

From this development it is possible to identify three different approaches to describe the TRI process. The most simple is the no-TRI approach, where $R_{T^4} = 1$ and $R_{I_b} = 0$, so where the TRI effects are ignored. In the partial TRI approach only the temperature auto-correlation is considered and $R_{I_b} = 0$, whereas in the full TRI approach both correlations are considered. These three approaches are evaluated and compared in the next sections.

3 Configuration and physical model

3.1 DNS calculation

Results of the direct numerical simulation (DNS) of a reactive turbulent flame are used for the TRI analysis. The data were provided by Jimenez [20], and reproduced the stabilization of a triple flame by inert hot gas. The flow configuration is a mixing layer of diluted methane (CH_4 20 % , N_2 80 % in volume) and air, as seen on Fig. 1. A hot gas layer is set above the air flow to stabilize the flame.
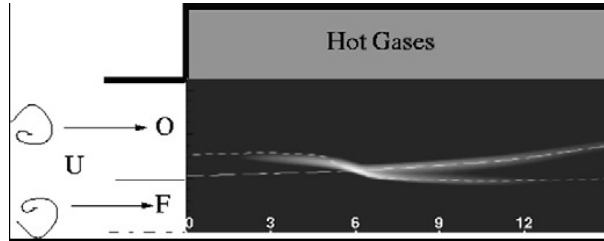

Figure 1: Simulation configuration and initial laminar flame. The rate of reaction is represented in levels of gray where the white represents the maximum. The lines represent the stoechiometric contour (long dash) and isotemperature line $T_i = T_0 + 0.5(T_{ad} - T_0)$ (short dash), where T_0 is the temperature for fresh gases and T_{ad} the adiabatic flame temperature.

The DNS are run by solving the fully compressible conservation equations for mass, momentum, energy and chemical species in a two dimensional Cartesian domain with a grid of 300 x 200 points, representing a physical space of 3 x 2 mm [20].

After the laminar flame is stabilized, turbulence is injected into the domain to obtain a turbulent flame (Fig. 2). The hot gas layer allows flame stabilization by the recirculation of hot gas. A zone of recirculation is created in the left higher corner, where the hot gas are trapped, providing the energy necessary to stabilize the flame (shown by the left arrow on Fig. 2), that otherwise would be convected downwards and finally blow off. The hot gas produced by

combustion are brought back by the recirculation towards the left higher corner to maintain the reserve of energy (right arrow on Fig. 2).
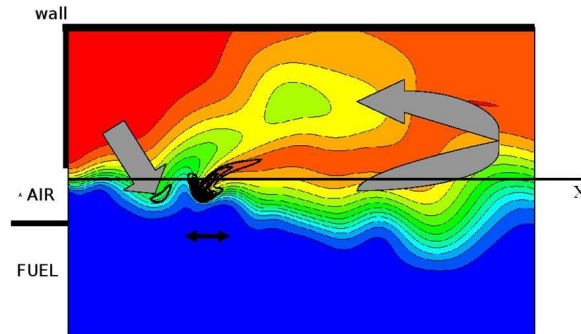

Figure 2: Instantaneous fields of temperature and isocontours of rate of reaction in the turbulent flame.

After sufficient time the average temperature remains constant, and the mean flow may be considered stationary, allowing to collect statistics (Fig. 3) .
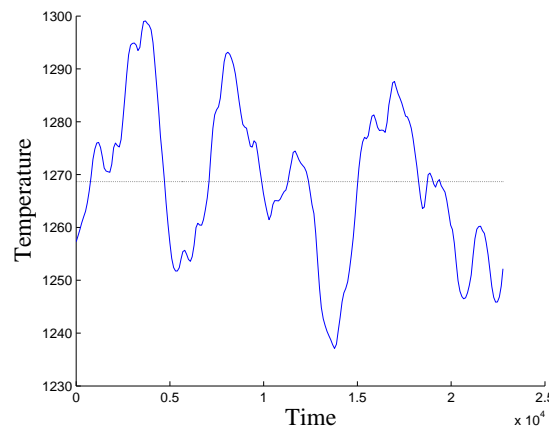

Figure 3: Evolution of the space mean temperature versus time.

The available data include density, velocity, total energy, mass fraction of the reactants (fuel and oxidant) as well as the temperature. These two last variables are used in our study to calculate the radiative terms in a post-processing approach.

3.2   TRI analysis

This study is performed in two steps. First, a diagnosis allows to evaluate the impact of filtering. Then modeling aspects are considered.

DNS results provide exact data for T and κ_P and give access to the exact emission $\kappa_P T^4$. DNS also allows to compute "exact" filtered quantities ($\overline{T}$, $\overline{\kappa_P}$, $\overline{T^4}$...) and fluctuations (T', κ'_P,...), as well as all types of correlations ($\overline{\kappa'_P T'}$,...). By definition, and supposing all assumptions valid, the full TRI approach should recover the "exact" filtered radiation terms.

In a LES only the filtered values of temperature and species concentrations are available but the filtered value of $\overline{T^4}$ or the correlation $\overline{\kappa'_P T'}$ for example are unknown. Models are therefore

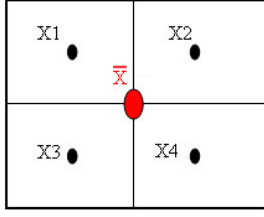needed to reconstruct them and DNS is used to evaluate and validate them.

Figure 4: Example of mesh filter

To reproduce the filter of a LES calculation, a box filter is applied to the DNS data as illustrated in Fig. 4. In this example the size of the filter is $2\Delta x$ (Δx being the mesh size of the uniform mesh used in DNS) and the filtered value is obtained by $\overline{X} = (X_1 + X_2 + X_3 + X_4)/4$.

More generally the expression of the filtered value at a node (i, j) is :

$$\overline{X_{ij}} = \frac{1}{N_{filt}^2} \sum_{k=i-N_{filt}/2}^{i+N_{filt}/2} \sum_{l=j-N_{filt}/2}^{j+N_{filt}/2} X_{kl} \tag{24}$$

where N_{filt}^2 is the number of cells involved. The filter size is $N_{filt}\Delta x$. The subgrid fluctuations are then given by the difference between the exact value (from the DNS) and the filtered value :

$$X'_{kl} = X_{kl} - \overline{X_{ij}} \tag{25}$$

The spatial mean over the whole domain of the intensity of fluctuation is then defined as:

$$I = \left\langle \frac{\sqrt{\overline{X'^2}}}{\overline{X}} \right\rangle \tag{26}$$

In a first step the analysis was done only along the central axis (in the longitudinal direction) of the configuration, where the fluctuations are most important and to better visualize the effects of filtering. In this case the filter operator is applied in the longitudinal direction only. The analysis of the total emission over the whole domain is made in a second step using a "box" filter as presented previously. Calculations were carried out for various filter sizes going from 1x1 Δx (i.e. no filter) to 100x100 Δx.

4 Results

4.1 Filtered data analysis

If the subgrid fluctuations are homogeneously distributed in the domain, the intensity I first increases with the filter size to reach a constant value after some point. If on the contrary there are important heterogeneities in the fluctuations, the intensity I also starts to increase with the filter size but may either continue to increase or decrease when heterogeneity is reached by the filtering box. In the studied case there are heterogeneities in temperature and species concentrations fluctuations, with important levels in the vicinity of the flame and much lower levels away from the flame. As shown on Fig. 5, these homogeneities are sufficient to modify the slope of the curve I versus N_{filt} but not to change its sign that stays always positive up to the maximum size filter.

On Fig. 6 the exact emission profile $\nabla \cdot q_{E,DNS}$ is shown along the central axis (see Fig. 2) and exhibits strong variations due to the presence of the flame. For comparison purposes, the exact filtered emission $\nabla \cdot q_{E,ref}$ (called the reference emission) as well as the emission resulting from the no-TRI, partial TRI and full TRI approaches are also plotted. As expected the full TRI approach is in exact agreement with the reference, demonstrating the validity of the assumptions made on the filter operator. However what is more surprising is that the no
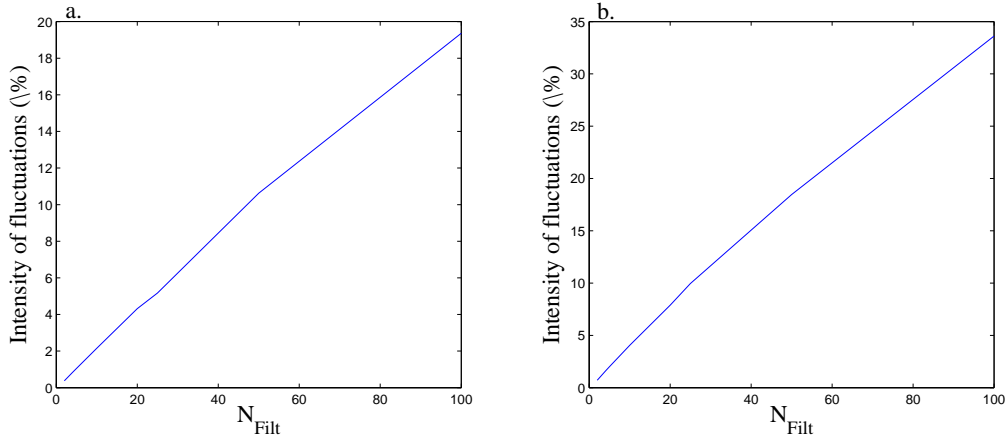
Figure 5: Fluctuation intensity, in percentage, of a. temperature, b. absorption coefficient, versus the filter size.

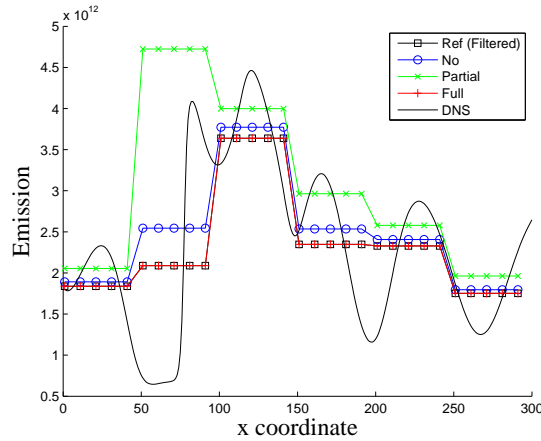TRI approach , although not as good as the full TRI, is by far much better than the partial TRI approach.

Figure 6: Emission profile along the flame axis for a filter of 50 Δx.

Fig. 7a shows the relative error along the flame axis, for different filter sizes, defined as :

$$\epsilon = \left\langle \left(\frac{\nabla \cdot q_E}{\nabla \cdot q_{E,ref}} - 1 \right) \times 100 \right\rangle \tag{27}$$

where the mean $\langle \rangle$ is taken along the axis. Also shown is the variance of the deviation from this mean value, represented by a vertical bar. The full TRI approach error is below 10^{-6} and even has a tendency to decrease when the filter size increases. On the contrary the no TRI and partial TRI approach show errors up to 10% and even higher for the latter. This is due to the sign of the correlation between the temperature and the absorption coefficient, that is negative in all present cases. The two correlations (R_{T^4} and R_{I_b}) have then opposite effects that are of the same order of magnitude and tend to compensate. Taking into account only one of them introduces therefore

large errors. In this case TRI should never be taken into account in a partial way but always in a complete way, including all terms of the development.
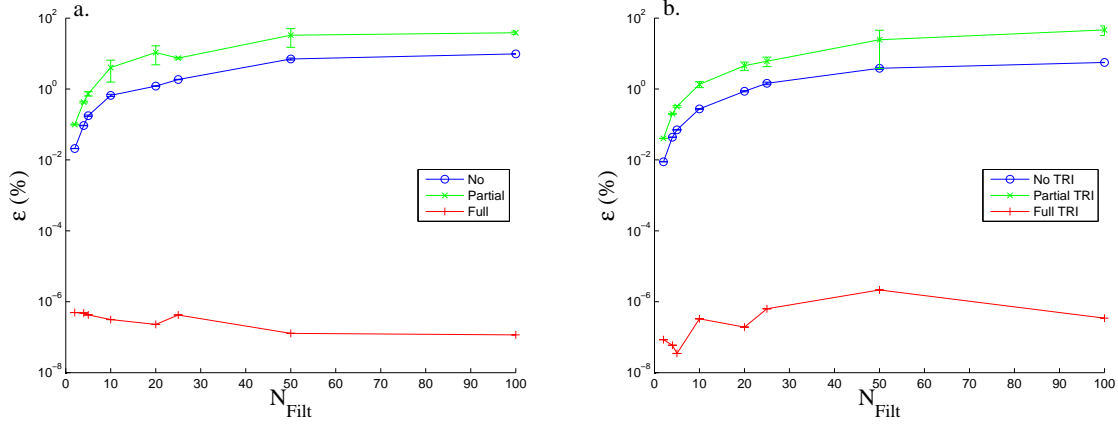

Figure 7: Relative error ϵ, a. along the axis of the flame, b. over the whole domain, versus the filter size for the various approaches.

The same analysis performed over the whole domain shows similar results and leads to the same conclusions, as seen on Fig. 7b where the error curves are very similar to the curves plotted along the flame axis.

4.2 Modeling

Taking into account the TRI implies then the reconstruction of both R_{T^4} and R_{I_b}. These correlations are not available in LES and need to be modeled. They may be evaluated from expressions (18) and (19), using the filtered temperature $\overline{T}$ and absorption coefficient $\overline{\kappa_P}$, and their subgrid scale fluctuations T' and κ'_P. However LES gives $\overline{T}$ but not T', and several approaches may be used to calculate it, that are largely presented in the literature and are not developed here. For the purpose of the present work, T' is directly reconstructed from the DNS data, as well as κ'_P and the other correlations of (19). This was done along the central axis for a 100 Δx filter. The relative error found on R_{I_b} is null, and is lower than 0,4% on R_{T^4}. This is not surprising as (18) and (19) are exact expressions of the correlations in the full TRI approach. The difficulty is in the evaluation of the above-mentionned subgrid scale variables, that are unknown in LES. In an attempt to reduce the number of unknown κ'_P-T' correlations and high order moments of temperature, terms of higher order than two have been dropped in (18) and (19). This led to an error lying between 0.1% and 1% on R_{T^4}, still acceptable, but between 3% and 9% on R_{I_b}. A first consideration towards LES modeling, expression (23) is tested. It requires the calculation of the term $\partial \kappa_P / \partial T$, that was evaluated with a simplified spectral model considering water emission only and the weighted sum of gray gas model. Results on the relative error are shown on Fig. 8.
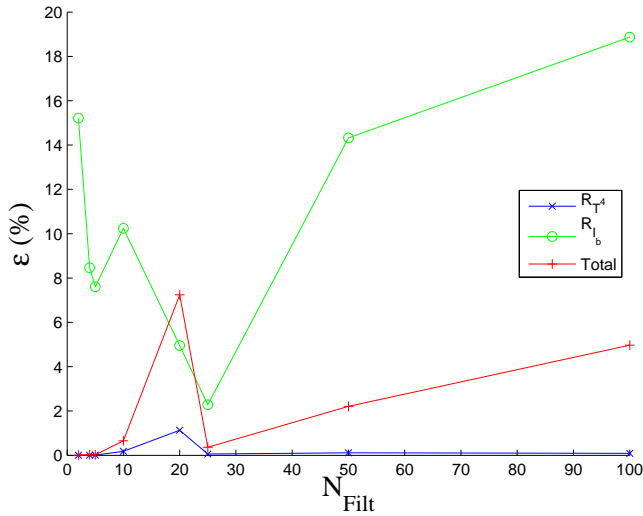
Figure 8: Relative error ϵ for the full TRI approch using expression (23), versus filter size.

A relatively important error on R_{I_b} appears for low values of the filter size, due to the fact that the dependence of κ_P with the species was neglected, and for large filter sizes, temperature fluctuations dominate. Adding the species dependency of κ_P allowed to decrease the error to few percents for the low values of the filter size, but increased the error for larger sizes (from 12% to 18%). The best result is obtained around a filter size of 20 Δx, corresponding to a filtering mesh size of 0.2 mm, which is the approximately one order of magnitude smaller than usual LES mesh sizes. This preliminary results give first trends for R_{T^4} and R_{I^b} modelling. Further analysis is needed to better understand the physical mechanisms and improve the models.

5   Conclusions

An *a priori* study was conducted from DNS of turbulent flames to characterize the influence of the various correlations that appear in the emission part of the radiative flux in the context of LES. The comparison between the exact and the filtered radiation emission calculated from the DNS and the same quantity calculated from the filtered data showed important discrepancies. Three approaches were defined in taking into account the various correlations in the radiation calculation: the no TRI ignores the correlations, the partial TRI involves the temperature auto-correlation only, and the full TRI adds the temperature/absorption coefficient correlation. As expected the full TRI is exact compared to the reference emission but the partial TRI approach performs worse than the no TRI approach. This shows that in the studied configuration, using only one of the two parts of the subgrid TRI is nonsense and that the full formulation should always be used. The effect of the filter size on the subgrid scale fluctuations is also investigated.

Simple models are evaluated to reconstruct the correlations in a LES framework. Results showed that if the dependency of the absorption coefficient with the species concentrations is included, good predictions may be obtained at small and moderate filter sizes. However all models failed for large filter sizes, in particular for the temperature-absorption coefficient correlation.

One major difficulty that was not addressed in the present paper is to evaluate subgrid scale variances and correlations needed by the radiation calculation and not directly available in a LES. This will be the next step of the present work, that will be now based on *a posteriori* analysis of LES calculations in both uncoupled and coupled way.

References

[1] J.P. Gore and G.M. Faeth. *Journal of Heat Transfer*, 110:173–181, 1988.

[2] M.E. Kounalakis, J.P. Gore, and G.M. Faeth. In *Proceedings of the Twenty-Second Symposium (International) on Combustion*, pages 1281–1290, 1988.

[3] M.E. Kounalakis, J.P. Gore, and G.M. Faeth. *Journal of Heat Transfer*, 111:1021–1030, 1989.

[4] J.P. Gore, S.M. Jeng, and G.M. Faeth. *Journal of Heat Transfer*, 109:165–171, 1987.

[5] J.P. Gore and G.M. Faeth. In *Proceedings of the Twenty-First Symposium (International) on Combustion*, pages 1521–1531, 1986.

[6] G. Cox. *Combustion Science and Technology*, 17:75–78, 1977.

[7] V.P. Kabashnikov and G.I. Kmit. *Journal Applied Spectroscopy*, 31(2):963–967, 1979.

[8] V.P. Kabashnikov and G.I. Myasiwkova. *Heat Transfer - Soviet Research*, 17(6):116–125, 1985.

[9] S.P. Burns. *SANDIA Report, SAND99-3190*, 1999.

[10] W.L. Grosshandler and P. Joulain. *Prog Aeronaut Astronaut*, 52(105-123), 1986.

[11] S.J. Fisher, B. Hardoiun-Duparc, and W.L. Grosshandler. *Combust Flame*, 70:291–306, 1987.

[12] S.M. Jeng and G.M. Faeth M.C. Lai. *Combust Sci Technol*, 40:41–53, 1984.

[13] Y. Zheng, Y.R. Sivathanu, and J.P. Gore. *Proc Comb Inst*, 29:1957–1963, 2002.

[14] Y. Zheng, R.S. Barlow, and J.P. Gore. *Journal of Heat Transfer*, 125(1065-1073), 2003.

[15] P.J. Coelho. *Combustion and Flame*, 136:481–492, 2004.

[16] B.R. Adams and P.J. Smith. *Comb Sci Technol*, 109:121–140, 2003.

[17] G. Li and M.F. Modest. *J Heat Transf*, 125:831–838, 2003.

[18] P.J. Coelho, O.J. Teerling, and D Roekaerts. *Comb Flame*, 133:75–91, 2003.

[19] Y. Wu, D.C. Haworth, M.F. Modest, and B. Cuenot. *Proc Combust Int*, 30:639–646, 2005.

[20] C. Jiménez and B. Cuenot. In The Combustion Institute, editor, *Proceedings of the combustion institute*, volume 31(I), pages 1649–1656, 2007.

[21] P. Chassaing. *Turbulence en Mécanique des fluides*. Cepadues, 2000.

[22] T. Poinsot and D. Veynante. *Theorical and Numérical Combustion*. Edwards, 2001.

[23] A. Soufiani and J. Taine. *Technical note in International Journal of Heat and mass transfer*, 40:987–991, 1997.

[24] F. Liu, G.J. Smallwood, and O.L. Gülder. *J Quant Spectrosc Radiative Transfer*, 68:401–417, 2001.

[25] D. Joseph. PhD thesis, Institut National Polytechnique de Toulouse, 2004.

[26] A. de Guilhem de Lataillade. PhD thesis, Institut National Polytechnique de Toulouse, 2001.